

AD-A067 794

GRUMMAN AEROSPACE CORP BETHPAGE N Y RESEARCH DEPT
IMPROVED TWO-MICRON CELESTIAL BACKGROUND ESTIMATES.(U)
MAR 79 D LEISAWITZ, J KRASSNER

F/G 3/1

UNCLASSIFIED

RM-682

NL

| OF |

AD
A067794

1

END
DATE
FILMED
6-79
DDC

RM-682

IMPROVED TWO-MICRON CELESTIAL
BACKGROUND ESTIMATES

March 1979

14
Grumman Research Department Memorandum RM-682

6 IMPROVED TWO-MICRON CELESTIAL BACKGROUND ESTIMATES.

by

9 Research memo.

10 David/Leisawitz and Jerry/Krassner
Nuclear and Astrophysics

12 27p.

DDC
RECEIVED
APR 16 1979
B

11 March 1979

Approved by *Richard A. Scheuing*
Richard A. Scheuing
Director of Research

DISTRIBUTION STATEMENT A
Approved for public release;
Distribution Unlimited

JOB

406 165

79 03 30 022

ABSTRACT

An improved galactic model is described that is used to predict contributions to the 2.2 micron (μm) background resulting from various classes of celestial objects. Initially, this model is fit to the Caltech Two-Micron Sky Survey to extrapolate to fluxes below the survey completeness level. Contributions to the 2.2 μm background due to main sequence stars and external galaxies -- not fully represented in the survey -- are shown to be significant at faint fluxes and are included in the model. Extinction from interstellar dust grains is also included and exhibits a considerable effect on the background at these fluxes. At brighter fluxes, the results of the improved model do not deviate significantly from those of the previous model. Several minor classes of objects have not been included in the predictions, and evidence is presented that their omission from the model has at most a minor effect on the total 2.2 μm background prediction. Suggestions are also made for future work.

ACCESSION for		
NTIS	White Section	<input checked="" type="checkbox"/>
DDC	Buff Section	<input type="checkbox"/>
UNANNOUNCED		<input type="checkbox"/>
JUSTIFICATION		
BY		
DISTRIBUTION/AVAILABILITY CODES		
Dist.	and/or	SPECIAL
A		

TABLE OF CONTENTS

<u>Section</u>	<u>Page</u>
Introduction.	1
Description of Galactic Models and Sources.	2
Previous Galactic Structure Model.	2
Modified Galactic Structure Model.	3
Extinction Modification.	6
Extragalactic Sources and Main Sequence Stars.	7
Results and Discussion.	12
Conclusions	18
References.	21

LIST OF ILLUSTRATIONS

<u>Figure</u>		<u>Page</u>
1	IRC Extrapolation Results for Ref. 1 and Present Models.	4
2	Number of Nonmain Sequence Sources (K Giant Stars and External Galaxies)/Square Degree Brighter Than 2.2 μm Flux H ($\text{W}/\text{cm}^2/\mu\text{m}$) vs H_λ	8
3	Number of Main Sequence Stars/Square Degree Brighter Than 2.2 μm Flux H ($\text{W}/\text{cm}^2/\mu\text{m}$) vs. H_λ	11
4	Celestial Background at 2.2 μm	13
5	Celestial Background at 2.2 μm vs Right Ascension for Various Limiting 2.2 μm Fluxes H	14

INTRODUCTION

This memorandum describes work recently completed to improve our representation of the celestial background at $2.2 \mu\text{m}$. A knowledge of this background is of interest to the defense community for problems in satellite navigation and remote sensing. In addition, such knowledge has scientific value for studies of stellar evolution and galactic structure. A model developed by Krassner et al. (Ref. 1) for extrapolation of the Caltech Two-Micron Sky Survey (Ref. 2) to fainter limiting fluxes (Ref. 2) has served as the foundation for this work. The IRC extrapolation model has been structurally modified so as to make it a more realistic representation of the true shape of our galaxy. In addition to accounting for extragalactic sources (as had been done in Ref. 1), two new factors are considered:

- The effect of faint main sequence stars not represented in the IRC
- The effect of interstellar extinction

Because these have opposing effects on the apparent source density, it was decided in Ref. 1 to neglect both factors as a first approximation. However, the present work has indicated that the main sequence contribution greatly outweighs the loss due to extinction effects, especially at faint limiting fluxes.

DESCRIPTION OF GALACTIC MODELS AND SOURCES

This section presents a review of the galactic structure model used in Ref. 1 that forms the starting point of the work reported here and describes modifications to this model that make it a more realistic representation of our galaxy. These modifications include the insertion of a radial taper to the galactic plane radial density law (which has the effect of excluding a galactic halo), the inclusion of interstellar reddening by modeling the galactic dust distribution, and the inclusion of main sequence stars in the analysis, which strongly affect the source counts at the fainter flux level considered.

PREVIOUS GALACTIC STRUCTURE MODEL

The Krassner et al. IRC extrapolation model (Ref. 1) gives the number of sources per steradian brighter than a limiting flux H_λ at $2.2 \mu\text{m}$:

$$\frac{dN}{d\Omega} (>H_\lambda) = -1/2 N(0,0) \int_0^{H_\lambda} \frac{R_c^2}{R_c^2 + R^2} e^{(-L_\lambda/H'_\lambda) (\sin B/\sigma)^2} L_\lambda^{3/2} H_\lambda'^{-5/2} dH'_\lambda \quad (1)$$

where

- $N(0,0)$ = galactic center density (sources/parsec³)
- R_c = characteristic radial scale of the density distribution in the galactic plane (parsecs)
- R = distance of star's projection on the galactic plane from the galactic center (parsecs)
- L_λ = source's intrinsic luminosity (parsecs² W/cm² μm)
- H_λ = source's apparent $2.2 \mu\text{m}$ irradiance as seen from earth (W/cm² μm)
- H'_λ = integration variable corresponding to H_λ
- B = galactic latitude
- σ = characteristic thickness of the galactic plane (parsecs)

Based on this model, a statistical analysis of the IRC was performed in Ref. 1, resulting in a matrix representation of the sky. The following best-fit values for the model parameters were obtained through an iterative process described in Ref. 1:

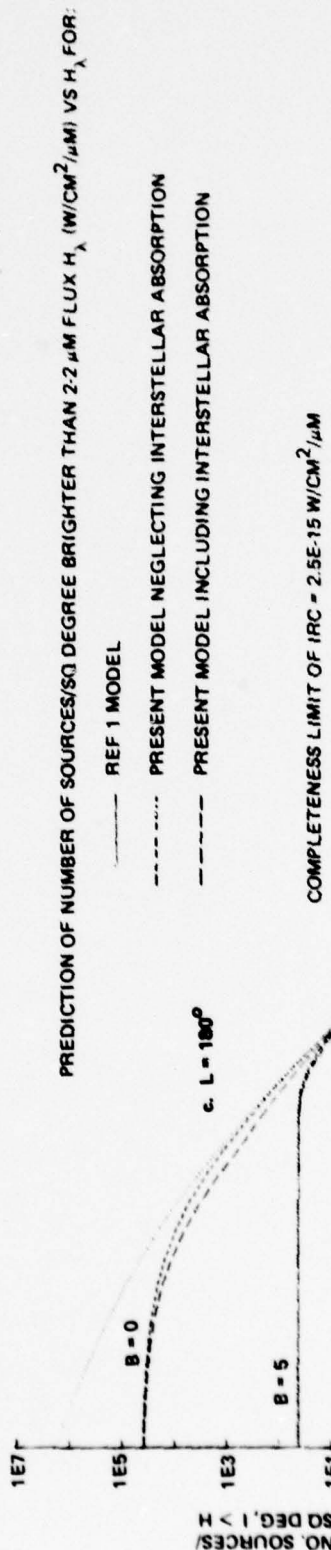
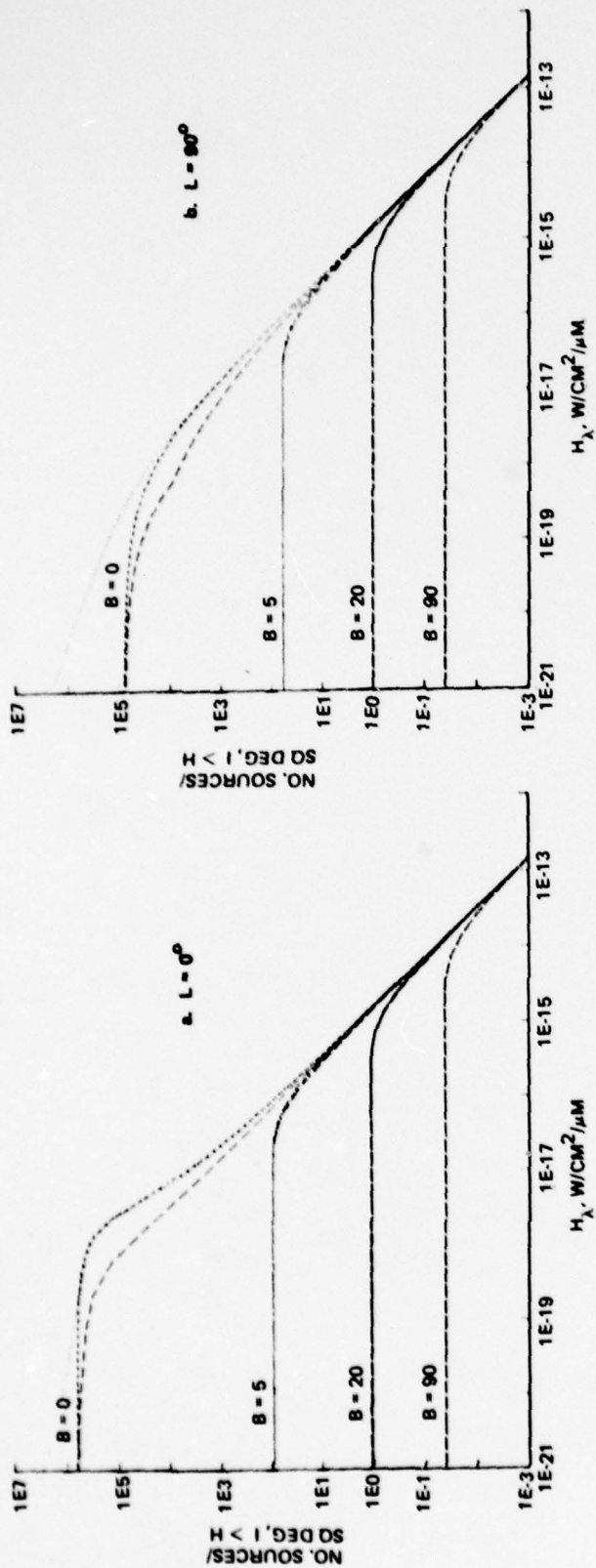
$$\begin{aligned}
 R_c &= 3000 \text{ parsecs} \\
 \sigma &= 130 \text{ parsecs} \\
 L_\lambda &= 2 \times 10^{-10} \text{ parsecs}^2 \text{ W/cm}^2 \mu\text{m} \\
 N(0,0) &= 0.0016 \text{ sources/parsec}^3 \\
 \text{Average error} &= 1.45 \text{ sources/matrix element}
 \end{aligned}$$

These parameters were found to be consistent with values derived by other astronomers.

MODIFIED GALACTIC STRUCTURE MODEL

The previous galactic model predictions agree with the IRC at brighter fluxes. However, in the galactic plane the extrapolation (see dotted lines on Fig. 1a-c) predicts an ever-increasing number of sources with fainter fluxes (a halo). For directions other than those in the galactic plane, the extrapolation has a different behavior: along these directions, the source density vs. limiting flux curves level off at fluxes corresponding to seeing to the galactic "edge" (no halo). Because the sensitivity limit of the IRC ($2.5 \times 10^{-15} \text{ W/cm}^2/\mu\text{m}$) implies an inability to detect stars further than several hundred parsecs distant, we have no information as to the existence of a galactic halo based on the IRC. However, this difference in behavior in and out of the plane is unsatisfactory. Faced with this difficulty, a choice was made to exclude the halo by inserting a radial taper in the galactic plane density law (see below). Justification for this choice is as follows:

- First, the existence of a halo of the type inferred here has not been unambiguously demonstrated by any astronomical observations to date
- Second, if such a halo were present, it would be noticeable only at the faintest fluxes considered here. At such fluxes other classes of objects, although minor by comparison to those already considered, are expected to be at least comparable and probably dominant to the halo
- Finally, even if the halo does exist, we do not know even the basic parameters needed to model its size, shape, and population.



PREDICTION OF NUMBER OF SOURCES/SQ DEGREE BRIGHTER THAN $2.2 \mu M$ FLUX H_A ($W/CM^2/\mu M$) VS H_A FOR:

- REF 1 MODEL
- - - PRESENT MODEL NEGLECTING INTERSTELLAR ABSORPTION
- . - PRESENT MODEL INCLUDING INTERSTELLAR ABSORPTION

Fig. 1 IRC Extrapolation Results for Ref. 1 and Present Models

With this in mind, a slight modification to the Ref. 1 model removes the halo in the plane. The galactic plane density law assumed in Ref. 1 is altered by including the factor $\frac{(15000)^2}{(15000^2 + R^2)}$ (suggested by Dr. T. Hilgeman, private communication). This is based on currently accepted estimates for a galactic radius of 15,000 parsecs and results in tapering the modeled galaxy to approximate a finite disc. For distances less than 15,000 parsecs from the galactic nucleus, this differs little from the previous model; beyond 15,000 parsecs, the disc is tapered as desired. The new IRC extrapolation model is thus:

$$\frac{dN}{d\Omega} (>H_\lambda) = -1/2N(0,0) \int_{-\infty}^{H_\lambda} \left[\frac{15000^2}{15000^2 + R^2} \right] \left[\frac{R_c^2}{R_c^2 + R^2} \right] e^{(-L_\lambda/H_\lambda') (\sin B/\sigma)^2} \times L_\lambda^{3/2} H_\lambda'^{-5/2} dH_\lambda' \quad (2)$$

The best-fit parameters obtained when the new model was applied to the IRC are:

$$R_c = 3700 \text{ parsecs}$$

$$\sigma = 130 \text{ parsecs}$$

$$L_\lambda = 2 \times 10^{-10} \text{ parsecs}^2 \text{W/cm}^2/\mu\text{m}$$

$$N(0,0) = 0.0016 \text{ sources/matrix element}$$

Only R_c is affected by the model alteration. Encouragingly, the resultant average error is comparable to that obtained in the Ref. 1 model.

Using the new set of parameters, the present model yielded the short-dashed curves in Fig. 1a-c. As expected, the old model results are reproduced for positions outside the galactic plane ($B \neq 0$), and the curves corresponding to lines of sight in the plane level off at limiting flux values corresponding to the edge of the galaxy.

EXTINCTION MODIFICATION

After we were satisfied that the new model was more precisely defined structurally, we proceeded with a consideration of interstellar extinction. The equation expressing apparent distance to an object (S_{app}) as a function of its actual distance (S_{act}) in the presence of absorption is:

$$S_{app}^2 = S_{act}^2 e^{-\kappa S_{act}} \quad (3)$$

in which κ is the wavelength dependent interstellar extinction coefficient. An accepted value for κ is 1.46×10^{-4} per parsec at $2.2 \mu m$ (Ref. 3), and this value is assumed below.

Furthermore, the apparent distance to an object is also expressible in terms of its intrinsic luminosity and measured irradiance as:

$$S_{app}^2 = L_{\lambda} / H_{\lambda meas} \quad (4)$$

Similarly, the actual distance is given in terms of the intrinsic luminosity and what would have been the irradiance had there been no extinction:

$$S_{act}^2 = L_{\lambda} / H_{\lambda} \quad (5)$$

From Eqs. (3), (4) and (5) we obtain:

$$H_{\lambda meas} = H_{\lambda} e^{-\kappa \sqrt{L_{\lambda} / H_{\lambda}}} = H_{\lambda} e^{-\kappa S_{act}} \quad (6)$$

Equation (3) contains no directional dependence whatsoever. The absorption model of Eq. (6) would therefore be unrealistic, for the interstellar grains responsible for absorption are concentrated in the galactic disc in what we may approximate by a flattened homogenous cylindrical dust cloud whose radius is 15 kiloparsecs (the assumed galactic radius) and whose thickness is 100 parsecs. Note that, in actuality, the grain distribution is quite clumpy. However, errors due to the assumption of homogeneity have their greatest effect over small patches of the sky. By modeling only the large scale structure of the sky, we effectively average these out. In addition, the problem only applies for nearby objects; at fainter fluxes, and hence larger distances, the clumpiness is averaged out.

The final form of the absorption model, after the isotropic Eq. (6) is slightly altered so as to introduce the homogeneous absorbing cylinder, is:

$$H_{\lambda \text{ meas}} = H_{\lambda} e^{-\kappa S_{\text{abs}}} \quad (7)$$

in which S_{abs} is the distance traversed through the absorbing cylinder along the line of sight to a source. For sources located within the cylinder, S_{abs} is simply the actual distance to the source, S_{act} , and Eq. (6) is applicable. For sources outside the cylinder, however, S_{abs} is less than S_{act} , and its value is given by the distance to the edge of the cylinder along the line of sight. To account for extinction effects, we need only shift the abscissa of the source density vs. limiting flux graphs according to Eq. (7).

The result of our consideration of absorption effects on the IRC extrapolation is clearly visible in Fig. 1a-c (long dashed lines). As expected, the most significant changes occur for lines of sight within the galactic plane, where the difference between S_{act} and S_{abs} is, on the average, relatively large. The effect of absorption decreases rapidly as $|B|$ increases from 0 (out of the galactic plane). In fact, even at $B = 20^\circ$, no absorption effects are discernible in our model.

Note that, independent of line of sight, the source densities obtained with and without extinction at a faint enough limiting flux eventually converge. This is to be expected since, regardless of amount of absorbing material, there must be some flux at which all sources in our galaxy will be seen (corresponding to seeing as far as the galactic "edge").

EXTRAGALACTIC SOURCES AND MAIN SEQUENCE STARS

In addition to the IRC class of sources, two other types of objects must be considered: extragalactic sources (i.e., external galaxies) and main sequence stars.

As has been previously mentioned, we have in Ref. 1 already accounted for the extragalactic contribution to the $2.2 \mu\text{m}$ celestial background according to the empirical equation:

$$\log N = -1.3 \log H - 24.1 \quad (8)$$

After applying our absorption model to this component of predicted source density and adding the result to the absorbed IRC extrapolation (long dashed lines), the solid lines in Fig. 2a-c result. Even at a limiting irradiance as low as

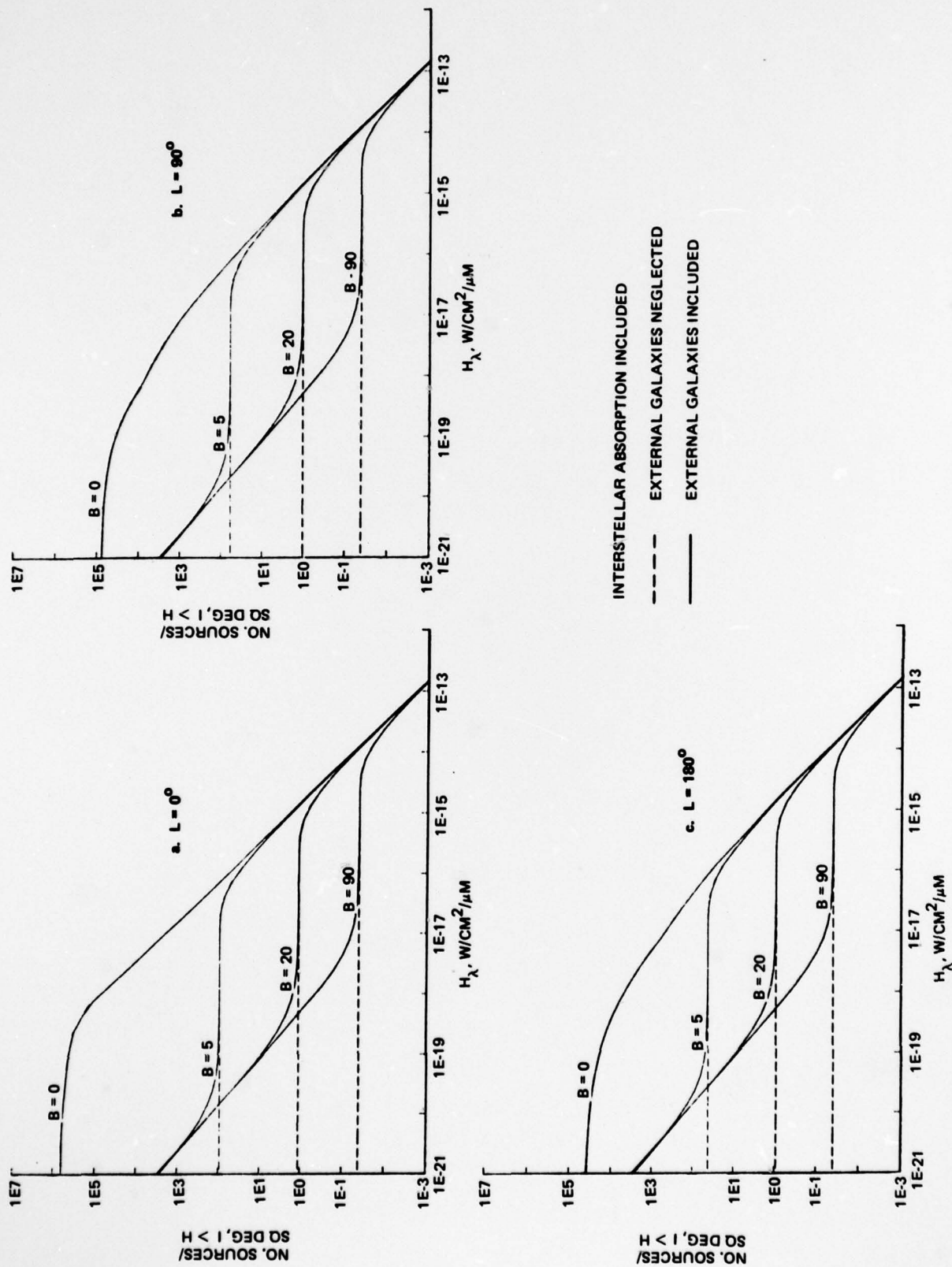


Fig. 2 Number of Nonmain Sequence Sources (K Giants Stars and External Galaxies)/Square Degree Brighter Than $2.2 \mu m$ Flux H ($W/cm^2/\mu m$) vs H_λ

$10^{-21} \text{W/cm}^2/\mu\text{m}$, the contribution due to external galaxies is seen to be negligible for lines of sight in the galactic plane, as is the case with the Ref. 1 model. Out of the plane, however, where absorption effects are less significant and IRC-type sources are less numerous, extragalactic sources dominate IRC sources, and the resultant curves are nearly identical to those obtained in Ref. 1.

The typical source observed in the IRC is a KIII (K giant) star with an effective black body temperature of approximately 3250°K . The mode of the IRC spectral type distribution occurs at type K5, in very good agreement with the best-fit luminosity. However, giant stars are greatly outnumbered by the less luminous main sequence stars in the galaxy. Hence, for faint limiting fluxes, we must also consider main sequence stars as potential $2.2 \mu\text{m}$ sources. Though most main sequence stars have effective radii too small to enable their corresponding infrared intrinsic luminosities to be comparable to K giants (which are about three orders of magnitude brighter), their overwhelming number density results in main sequence stars being the dominant $2.2 \mu\text{m}$ emitters at faint enough limiting fluxes. The following data for main sequence stars were obtained from Ref. 4:

TABLE 1 PROPERTIES OF MAIN SEQUENCE STARS

Spectral Type	O	B	A	F	G	K	M
$\sigma(\text{parsecs})$	50	60	115	190	340	350	350
$N(\text{solar})$ (parsec^{-3})	2×10^{-8}	$1 \times 10^{-5*}$	5.7×10^{-4}	2.2×10^{-3}	4.3×10^{-3}	1×10^{-2}	6.5×10^{-2}
M_K	-4.5	-2.0*	+1.2*	+2.0*	+3.5*	+4.2*	+6.0*

* Estimated. Several values were given corresponding to different spectral subclasses.

In Table 1, σ is the characteristic thickness of the galaxy for stars of the indicated spectral type; $N(\text{solar})$ is their source density in the solar neighborhood; and M_K is their typical absolute magnitude at $2.2 \mu\text{m}$.

By the definition of K magnitude, we may use the following formula to convert the $2.2 \mu\text{m}$ absolute magnitudes, M_K , from Table 1 to intrinsic luminosities at $2.2 \mu\text{m}$:

$$L(2.2\mu\text{m}) = (4 \times 10^{-12})(2.512)^{-M_K} (\text{parsecs}^2 \text{W/cm}^2/\mu\text{m}) \quad (9)$$

Source density at the galactic center, $N(0,0)$, may be expressed in terms of the solar neighborhood density using the modified galactic plane density law:

$$N(0,0) = \left(\frac{3700^2 + R_\odot^2}{3700^2} \right) \left(\frac{15000^2 + R_\odot^2}{15000^2} \right) N(\text{solar}) \approx 12 N(\text{solar}) \quad (10)$$

where for R_\odot , the sun's distance from the galactic center, we use the currently accepted value of 10 kiloparsecs.

The above values for σ are given along with calculated values of galactic center source density and intrinsic luminosity in Table 2:

TABLE 2 MODEL PARAMETERS FOR MAIN SEQUENCE STARS

Spectral Type	O	B	A	F	G	K	M
(parsecs)	50	60	115	190	340	350	350
$N(0,0)$ (parsecs ⁻³)	2.4×10^{-7}	1.2×10^{-4}	6.8×10^{-3}	0.026	0.052	0.12	0.78
$L(2.2\mu\text{m})$ parsecs ² W/cm ² /μm	2.5×10^{-10}	2.5×10^{-11}	1.2×10^{-11}	6.4×10^{-13}	1.6×10^{-13}	8.4×10^{-14}	1.6×10^{-14}

The IRC doesn't contain enough main sequence stars to fit galactic parameters. Therefore, we have retained our value of 3700 parsecs for the characteristic radial scale of the density distribution in the galactic plane. Though it was obtained from a statistical sample of primarily giant stars, we assume this value to be generally applicable. We therefore have four parameters (R_c , σ , $N(0,0)$, and L_λ) for each main sequence spectral type that may be substituted in the galactic (extrapolation) model, Eq. (2).

Because a different luminosity corresponds to each spectral type, our absorption model must be applied to each type individually prior to summing to obtain the overall main sequence contribution to the 2.2 μm celestial background. Source density vs. limiting flux has been plotted for the main sequence stars both with and without absorption in Fig. 3a-c.

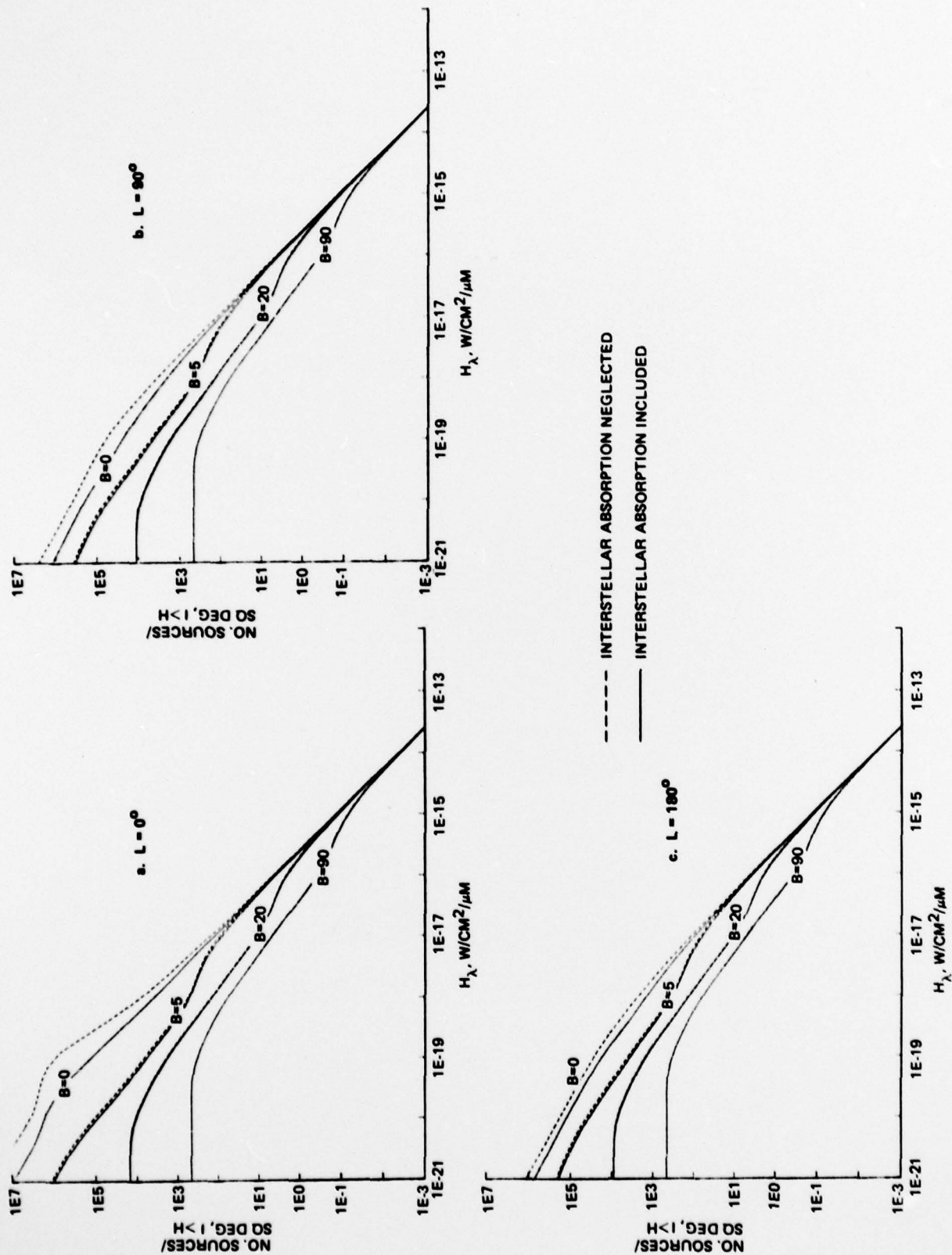


Fig. 3 Number of Main Sequence Stars/Square Degree Brighter Than $2.2 \mu\text{m}$ Flux H ($\text{W}/\text{cm}^2/\mu\text{m}$) vs H_λ

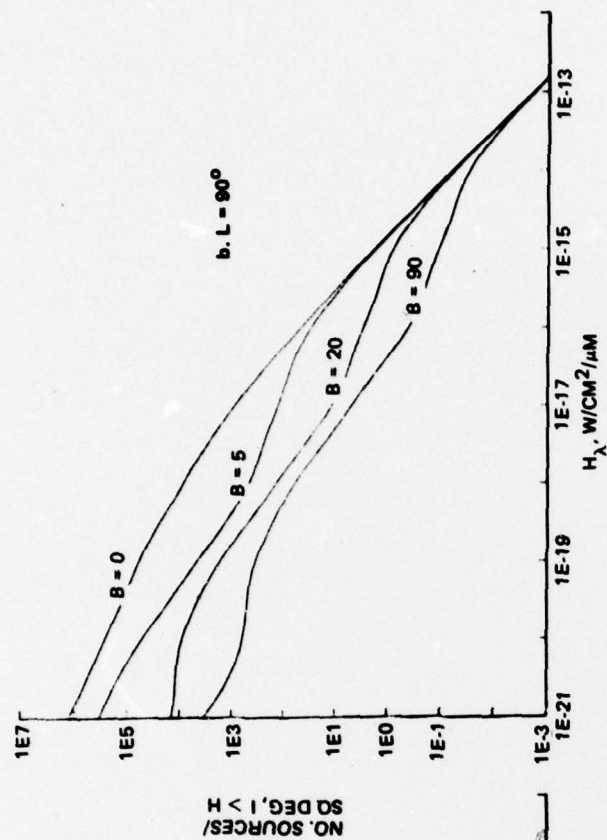
RESULTS AND DISCUSSION

By summing the contributions due to main sequence (Fig. 3a-c) and nonmain sequence (Fig. 2a-c) sources in the presence of absorption, we obtain an improved prediction of the $2.2 \mu\text{m}$ celestial background (Fig. 4a-c). Careful inspection reveals a similar component structure along each of the 12 lines of sight considered. At the brightest limiting flux values, the contribution in each direction is due primarily to IRC-type (K giant) sources. This is also true of the Ref. 1 predictions and is expected. Main sequence stars dominate the source density for moderately faint fluxes, while extragalactic sources make their presence apparent at the very faintest limiting irradiances considered.

As the line of sight approaches the galactic plane, main sequence stars become less and less dominant. For instance, over the flux range from 10^{-16} to about $3 \times 10^{-20} \text{ W/cm}^2/\mu\text{m}$, the graph for $L = 0$, $B = 90^\circ$ in Fig. 4a has an appearance identical to that of the corresponding line of sight in Fig. 3a, indicating the dominance of main sequence sources. However, at $L = 0$, $B = 0$ (toward the galactic center), no main sequence component is visible except at the faintest limiting flux considered ($10^{-21} \text{ W/cm}^2/\mu\text{m}$).

With extinction and main sequence stars accounted for, the contribution to the $2.2 \mu\text{m}$ celestial background due to extragalactic sources has negligible effect except for lines of sight nearly perpendicular to the galactic plane, and then only for flux limits below $10^{-20} \text{ W/cm}^2/\mu\text{m}$.

In addition to galactic latitude and longitude, our results may alternatively be presented in celestial coordinates (right ascension and declination). Three declination bands ($+10^\circ$, 0° , and -10°) are chosen, and for each limiting flux H_λ , the number of sources per square degree with irradiance brighter than H_λ are plotted as a function of right ascension (see Fig. 5a-c). The peaks centered around right ascension $\alpha(1950.0) \approx 7^{\text{h}}$ correspond to crossing the galactic plane at galactic longitude $L \approx 215^\circ$, and the peaks centered at $\alpha(1950.0) \approx 19^{\text{h}}$ correspond to passing through the plane at $L \approx 33^\circ$. At the declinations considered, the galactic center ($L = 0$, $B = 0$), anticenter ($L = 180^\circ$, $B = 0$), and poles ($B = \pm 90$) are not represented. Referring to Figs. 2 through 4, it can be shown that Fig. 5a depicts primarily IRC giant sources, Fig. 5c represents



TOTAL NUMBER OF SOURCES/SQ. DEGREE BRIGHTER
THAN $2.2 \mu m$ FLUX H_λ ($W/CM^2/\mu m$) VS. H_λ FOR ALL
OBJECTS CONSIDERED

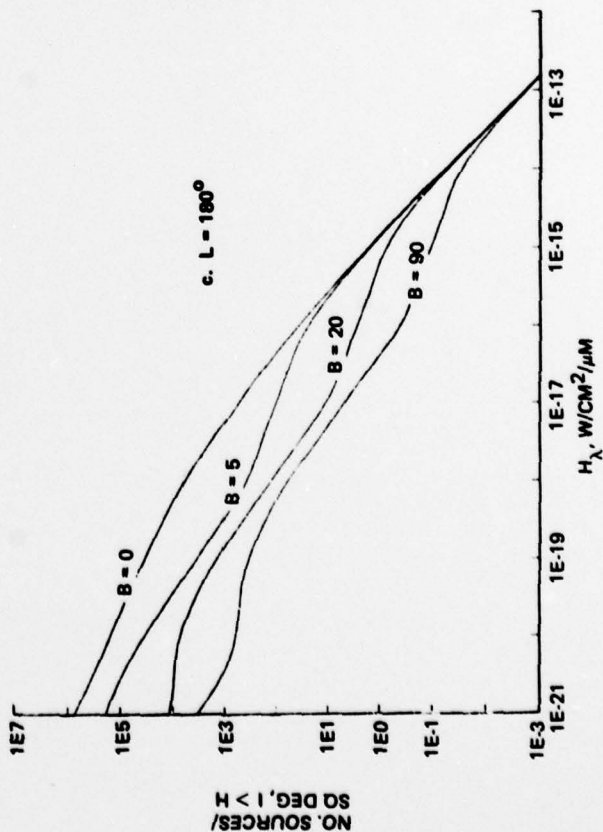


Fig. 4 Celestial Background at $2.2 \mu m$

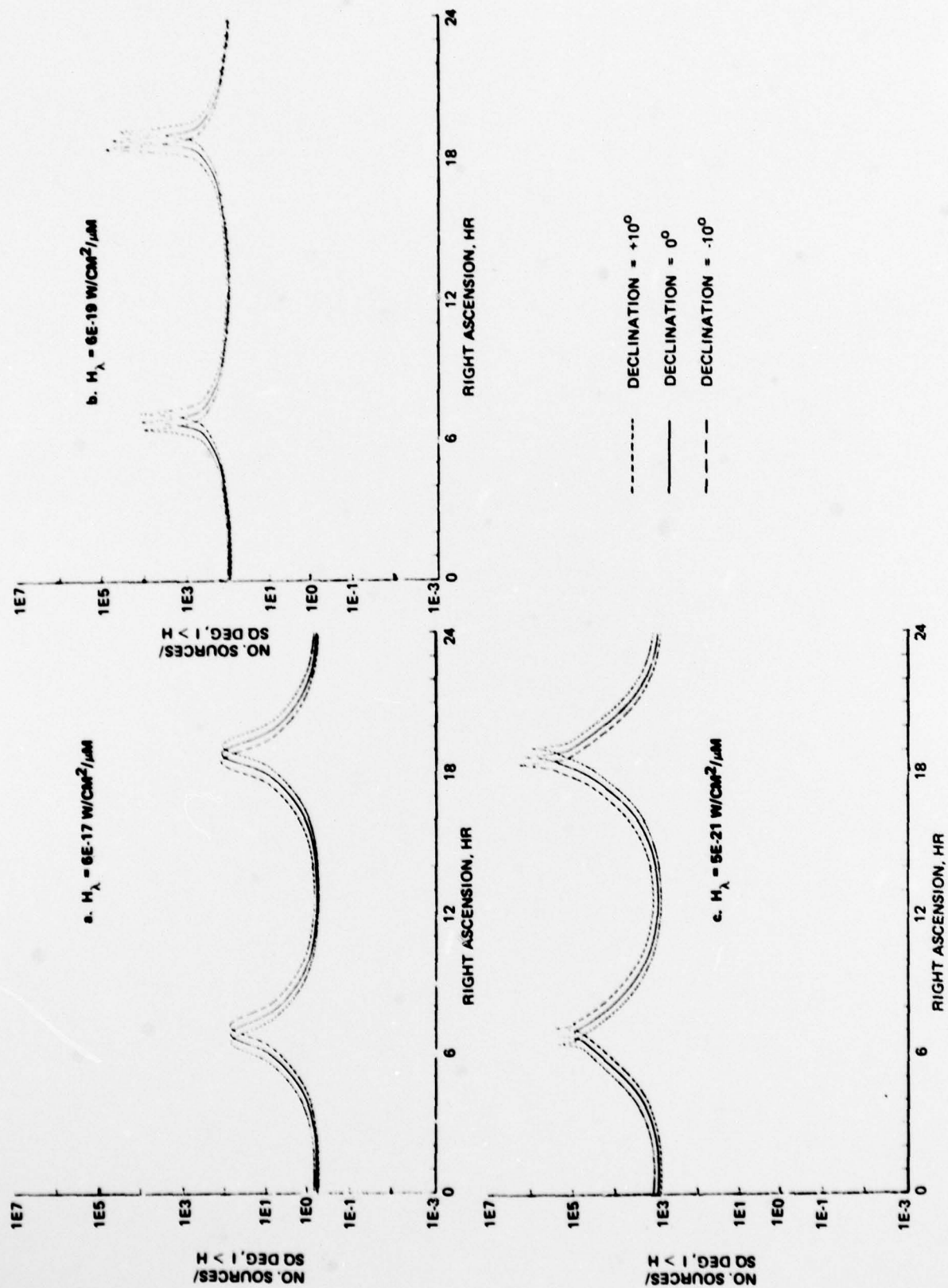


Fig. 5 Celestial Background at $2.2 \mu\text{m}$ vs Right Ascension for Various Limiting $2.2 \mu\text{m}$ Fluxes H_α

primarily main sequence stars, and Fig. 5b is an intermediate case with giants dominating the peaks and main sequence stars dominating elsewhere. Features observed in these figures -- such as peak sharpening, flattening of the region between peaks, and full widths of the peaks at half maxima (FWHM) -- are explained in terms of absorption and the shape of the galaxy. The apparent shape of the galaxy, in turn, depends upon what component of source density is dominant at a particular limiting irradiance because to each component there corresponds a different σ ; that is, in our galactic model, the distance-from-plane dependence of source density is included in the gaussian:

$$e^{-(S_{\text{act}} \sin B / \sigma)^2} \quad (11)$$

For $H_\lambda = 6 \times 10^{-17} \text{ W/cm}^2/\mu\text{m}$, IRC-type sources dominate the $2.2 \mu\text{m}$ celestial background at all but the highest galactic latitudes, where main sequence sources dominate. With this H_λ and an intrinsic luminosity of $2 \times 10^{-10} \text{ parsecs}^2 \text{ W/cm}^2/\mu\text{m}$ (from the IRC parameter fit), Eq. (4) implies an apparent distance of 1800 parsecs. Because of absorption effects, this corresponds to an even smaller actual distance of about 1600 parsecs. Relative to an observing range of 1600 parsecs, a galactic thickness of 130 parsecs is quite significant. We are therefore justified in concluding that at $6 \times 10^{-17} \text{ W/cm}^2/\mu\text{m}$ the galactic plane appears to subtend a relatively large angular diameter, thus accounting for a fairly large FWHM for the peaks in Fig. 5a. Their shape is, of course, determined by the aforementioned gaussian distribution (Eq. (11)) in which a value of 130 parsecs is used for σ .

At the fainter limiting flux of $6 \times 10^{-19} \text{ W/cm}^2/\mu\text{m}$ (Fig. 5b) main sequence stars outnumber giants as well as external galaxies along all lines of sight except for those very near the plane. Now, however, with a limiting flux two orders of magnitude fainter, we are able to detect IRC sources in the galactic disc to actual distances greater than 9000 parsecs at $L = 33^\circ$ and to nearly 12,000 parsecs at $L = 215^\circ$. A greater distance is obtained at $L = 215^\circ$ because of the truncation of absorption at the edge of the galaxy. The galactic edge in this direction is 5600 parsecs away, about half as distant as the actual observing range. Once again, the effective galactic thickness (as determined for IRC-type sources) is 130 parsecs, but at these great distances the galactic plane is confined to an angular thickness much smaller than that determined for $H_\lambda = 6 \times 10^{-17} \text{ W/cm}^2/\mu\text{m}$. Our resolution of galactic structure has therefore been

significantly enhanced, enabling us to account for the small FWHM values for the peaks in Fig. 5b. As a consequence of the angular thinness of the peaks, the gaussian defining the peaks appears pointed. In other words, at this value of H_λ , the model detects galactic sources to a distance of 9 kpc in the direction $L = 33^\circ$, $B = 0^\circ$ while only to 5.6 kpc in the direction $L = 215^\circ$, $B = 0^\circ$; this accounts for the peaks at $\alpha \sim 7^h$ being slightly shorter and having a slightly larger FWHM than those at $\alpha \sim 19^h$.

At $H_\lambda \approx 5 \times 10^{-21} \text{ W/cm}^2/\mu\text{m}$, main sequence sources are dominant along all lines of sight. Along these lines of sight corresponding to the peaks in Fig. 5c, main sequence stars of spectral type A contribute most significantly to the source density. These stars have a characteristic galactic thickness of 115 parsecs and their luminosity enables us to detect them to distances as great as 14 kiloparsecs toward $L = 33^\circ$, $B = 0$ and to more than 25 kiloparsecs toward $L = 215^\circ$, $B = 0$, thereby accounting for the sharpness of the peaks. The peak corresponding to a galactic longitude of 33° is noticeably higher and thinner than the peak associated with $L = 215^\circ$. This is because galactic sources along $L = 33^\circ$ may be detected as far away as 14 kiloparsecs as determined by absorption, the flux limit, and the effective luminosity; at $L = 215^\circ$ the galactic "edge" is only about 5700 parsecs distant, and this determines a limit to the number of observable sources (external galaxies do not yet contribute significantly). At $H_\lambda = 5 \times 10^{-21} \text{ W/cm}^2/\mu\text{m}$, the next most abundant class of stars are F and then G main sequence stars. Each has a successively larger σ , which accounts for the broadness of the peaks.

As expected the overall source density increases with fainter and fainter flux limits (progression from Fig. 5a-c); it is, however, worth noting that although source density increases by two orders of magnitude for a decrease of two orders of magnitude in H_λ from 6×10^{-17} to $6 \times 10^{-19} \text{ W/cm}^2/\mu\text{m}$, the source density goes up only about one order of magnitude when the limiting flux is decreased by nearly two more orders of magnitude to $5 \times 10^{-21} \text{ W/cm}^2/\mu\text{m}$. Again, this effect is primarily attributable to absorption, the galactic "edge," and an effective galactic thickness. For lines of sight out of the plane, different components dominate to different limiting fluxes because some sources are typically found further from the galactic plane than others. For a given line of sight in the disc and a given class of stars, absorption becomes increasingly significant for fainter and fainter irradiance limits. Also, at faint enough

fluxes, observation to actual distances surpassing that of the galactic "edge" are possible, resulting in a temporary (until extragalactic sources are detectable) cutoff in the number of sources observed.

CONCLUSIONS

The Ref. 1 predictions for the $2.2\ \mu\text{m}$ source densities were based on K giant stars along all lines of sight down to the fluxes at which the effects of external galaxies become important. At all but the faintest fluxes considered, we still estimate that giant stars outnumber all others for lines of sight in the galactic plane. However, the structural modification to the model (Eq. (2)) and considerations of interstellar absorption both have significant effects in the plane. For fainter stars, along lines of sight outside the galactic plane, we have determined a main sequence star dominance. As a net result, the present predictions differ from those given in Ref. 1 along all lines of sight for the fainter flux limits.

Further refinements to the celestial background prediction could include consideration of additional sources, statistical studies of moments of the distribution (clumping), and extrapolation to other wavelengths. Some of the additional sources which could be considered are HII regions, supernova remnants, planetary nebulae, variable stars, and subdwarfs. As noted in the following paragraphs, we do not expect these sources to be significant for the present work. The existence of clumping is evident in visual data, showing up in clusters, binary stars, and apparent projection effects. Extrapolation to other wavelengths would be useful for evaluating other catalogs as well as for providing a good estimate of the densities of fainter sources at these wavelengths.

Rough estimates of the contributions of each of the above additional objects to the total source count can be made. HII regions are associated with, and have at most a luminosity equaling that of O and B stars. Since the O and B stars produce a negligible contribution to the main sequence counts, HII regions will be equally negligible. Supernova remnants, although extremely luminous, are very rare. (The Crab nebula has an absolute $2.2\mu\text{m}$ luminosity comparable to the IRC giant stars.) Assuming a generous supernova rate of a $\sim 5/\text{century}$ and a lifetime of $\sim 10^5$ years implies ~ 5000 supernova remnants in the galaxy at a given time. Hence, in spite of their large luminosities, supernova remnants are too rare to be important when compared to the $\sim 10^{11}$ galactic giant

and main sequence stars. Planetary nebulae have $2.2 \mu\text{m}$ luminosities about 20 percent that of giant stars. However, their assessed number density in the galaxy is ~ 1 percent that of the giant stars. The combination of lower luminosities and fewer sources again results in their not contributing significantly to the total source counts. Though the luminosities of the brightest classes of variable stars are comparable to those of giants, their extremely small number density compared to main sequence stars ($\sim 10^{-7}/\text{parsec}^3$ compared to $\sim 10^{-2}/\text{parsec}^3$ in the solar neighborhood) again justifies our having neglected this group. The same conclusion is true for subdwarf stars, especially given that their luminosity is ~ 5 times less than that of the more prevalent main sequence stars (K and M types).

Clumping is commonly observed among stars in the galaxy. A number of phenomena are responsible for this effect, including actual clustering of stars into groups of varying size (e.g., globular clusters), the tendency of stars to form in "open clusters" and in pairs (binary stars), and projection effects in which several unrelated stars might be along almost identical lines of sight (although at different distances). Furthermore, because a detector sees a finite field of view, several faint stars (just below the detector's threshold for detection) might not be spatially resolved, but their combined flux could cause a response by the detector. The degree of clumping would have an effect on the rate of such false detections. This effect has been known to radio astronomers for many years as the "confusion limit." A statistical analysis of clumping (determining moments of the source distribution function) would be needed to analyze this effect.

Extrapolation of the present model to longer or shorter wavelengths could be more realistic than predictions based on fits to other catalogs. This is because the IRC is complete to distances sufficient to resolve galactic structure and has a large number of sources, most of which are similar in luminosity. Visual catalogs are complete only in the solar neighborhood due to the effects of interstellar extinction, which varies with viewing direction. Existing longer wavelength catalogs lack a sufficient number of sources for reliable statistics and include a variety of unidentified sources of presumably widely varying luminosity.

In summary, we believe that the present source density predictions are an improvement over those of Ref. 1 at faint flux levels. In addition, we have indicated other classes of objects that could be detectable at faint fluxes and

have presented reasons why their inclusion in the present model would produce at most minor changes. As a result, it is our feeling that a fruitful area for future work would be to concentrate on the clumping and the wavelength extrapolation aspects of the problem of determining the celestial background.

REFERENCES

1. Krassner, J., Hilgeman, T., and Brissenden, M., "Celestial Background at 2.2 Micron," Grumman Research Department Memorandum (RM-675), January 1979.
2. Neugebauer, G., and Leighton, R.B., "Two-Micron Sky Survey - A Preliminary Catalog," NASA SP-3047, 1969.
3. Johnson, H.L., in "Nebulae and Interstellar Matter," (Vol. III of Stars and Stellar Systems), G. Kuiper, ed., University of Chicago Press, 1968.
4. Hughes, E., "The Luminosities and the Spatial Distribution of Stars Detected on a Two Micron Sky Survey," Ph.D. Thesis, California Institute of Technology, 1968.

UNCLASSIFIED

SECURITY CLASSIFICATION OF THIS PAGE (When Data Entered)

REPORT DOCUMENTATION PAGE		READ INSTRUCTIONS BEFORE COMPLETING FORM
1. REPORT NUMBER RM-682	2. GOVT ACCESSION NO.	3. RECIPIENT'S CATALOG NUMBER
4. TITLE (and Subtitle) Improved 2-Micron Celestial Background Estimates		5. TYPE OF REPORT & PERIOD COVERED Research
7. AUTHOR(s) David Leisawitz & Jerrk Krassner		6. PERFORMING ORG. REPORT NUMBER RM-682
9. PERFORMING ORGANIZATION NAME AND ADDRESS Research Department Grumman Aerospace Co., Bethpage, NY 11714		8. CONTRACT OR GRANT NUMBER(s)
11. CONTROLLING OFFICE NAME AND ADDRESS		10. PROGRAM ELEMENT, PROJECT, TASK AREA & WORK UNIT NUMBERS
14. MONITORING AGENCY NAME & ADDRESS (if different from Controlling Office)		12. REPORT DATE March 1979
		13. NUMBER OF PAGES 21
		15. SECURITY CLASS. (of this report)
		15a. DECLASSIFICATION/DOWNGRADING SCHEDULE
16. DISTRIBUTION STATEMENT (of this Report) Approved for Public Release; Distribution Unlimited		
17. DISTRIBUTION STATEMENT (of the abstract entered in Block 20, if different from Report)		
18. SUPPLEMENTARY NOTES		
19. KEY WORDS (Continue on reverse side if necessary and identify by block number) Celestial Background, Sky Survey, Extragalactic, Sequence Stars, K Giants, Infrared		
20. ABSTRACT (Continue on reverse side if necessary and identify by block number) A knowledge of the infrared celestial background is of interest to the defense community for problems in satellite navigation and remote sensing. In addition, such knowledge has scientific value for studies of stellar evolution and galactic structure. Using an improved galactic model in our computer code CELES, we predict the contribution to the 2.2-micron background due to various classes of celestial objects.		

DD FORM 1 JAN 73 1473

EDITION OF 1 NOV 65 IS OBSOLETE
S/N 0102-014-6601

UNCLASSIFIED

SECURITY CLASSIFICATION OF THIS PAGE (When Data Entered)